

## RESEARCH ARTICLE

# Apical CLC-2 in retinal pigment epithelium is crucial for survival of the outer retina

Christin Hanke-Gogokhia<sup>1</sup> | Guillermo L. Lehmann<sup>2</sup> | Ignacio Benedicto<sup>3</sup> |  
 Erwin de la Fuente-Ortega<sup>4</sup> | Vadim Y. Arshavsky<sup>5</sup> | Ryan Schreiner<sup>6</sup>  |  
 Enrique Rodriguez-Boulan<sup>7</sup> 

<sup>1</sup>Department of Ophthalmology, Yale University, New Haven, CT, USA

<sup>2</sup>Regeneron Pharmaceuticals, Inc., Tarrytown, NY, USA

<sup>3</sup>Centro Nacional de Investigaciones Cardiovasculares (CNIC), Madrid, Spain

<sup>4</sup>Departamento de Ciencias Biomédicas, Facultad de Medicina, Universidad Católica del Norte, Coquimbo, Chile

<sup>5</sup>Department of Ophthalmology, Duke University School of Medicine, Durham, NC, USA

<sup>6</sup>Division of Regenerative Medicine, Ansbary Stem Cell Institute, Department of Medicine, Weill Cornell Medicine, New York, NY, USA

<sup>7</sup>Department of Ophthalmology, Margaret Dyson Vision Research Institute, Weill Cornell Medicine, New York, NY, USA

## Correspondence

Ryan Schreiner and Enrique Rodriguez-Boulan, 1300 York Ave, New York, NY 10065, USA.  
 Emails: rps2001@med.cornell.edu; boulan@med.cornell.edu

## Funding information

HHS | NIH | National Eye Institute (NEI), Grant/Award Number: EY08538; HHS | NIH | National Institute of General Medical Sciences (NIGMS), Grant/Award Number: GM34107; New York State Stem Cell Science (NYSTEM), Grant/Award Number: C32596GG; Comunidad de Madrid, Grant/Award Number: 2017-T1/BMD-5247; MINECO | Instituto de Salud Carlos III (ISCIII); Ministerio de Ciencia e Innovación (MICINN); Weill Cornell Medicine, Grant/Award Number: EY005722

## Abstract

Knockout of the chloride channel protein 2 (CLC-2; CLCN2) results in fast progressing blindness in mice. Retinal Pigment Epithelium (RPE) and photoreceptors undergo, in parallel, rapid, and profound morphological changes and degeneration. Immunohistochemistry and electron microscopy of the outer retina and electroretinography of the CLC-2 KO mouse demonstrated normal morphology at postnatal day 2, followed by drastic changes in RPE and photoreceptor morphology and loss of vision during the first postnatal month. To investigate whether the RPE or the photoreceptors are the primary cause of the degeneration, we injected lentiviruses carrying HA-tagged CLC-2 with an RPE-specific promoter in the subretinal space of CLC-2-KO mice at the time of eye opening. As expected, CLC-2-HA was expressed exclusively in RPE; strikingly, this procedure rescued the degeneration of both RPE and photoreceptors. Light response in transduced eyes was also recovered. Only a fraction of RPE was transduced with the lentivirus; however, the entire RPE monolayer appears healthy, even the RPE cells not expressing the CLC-2-HA. Surprisingly, in contrast with previous physiological observations that postulate that CLC-2 has a

**Abbreviations:** 1M, one month; CLC-2, chloride channel protein 2; DMEM, Dulbecco's modified Eagle medium; ERG, electroretinogram; FBS, fetal bovine serum; HA, hemagglutinin; hFRPE, human fetal retinal pigment epithelium; INL, inner nuclear layer; IS, inner segment; KO, knock-out; NKCC, sodium potassium chloride co-transporter; ONL, outer nuclear layer; OS, outer segment; P2, postnatal day two; P7, postnatal day seven; P12, postnatal day twelve; P14, postnatal day fourteen; PBS, phosphate buffered saline; PCR, polymerase chain reaction; PDGF, platelet-derived growth factor; RPE, retinal pigment epithelium; RT, room temperature.

This is an open access article under the terms of the Creative Commons Attribution-NonCommercial-NoDerivs License, which permits use and distribution in any medium, provided the original work is properly cited, the use is non-commercial and no modifications or adaptations are made.

© 2021 The Authors. *The FASEB Journal* published by Wiley Periodicals LLC on behalf of Federation of American Societies for Experimental Biology.

basolateral localization in RPE, our immunofluorescence experiments demonstrated CLC-2 has an apical distribution, facing the subretinal space and the photoreceptor outer segments. Our findings suggest that CLC-2 does not play the postulated role in fluid transport at the basolateral membrane. Rather, they suggest that CLC-2 performs a critical homeostatic role in the subretinal compartment involving a chloride regulatory mechanism that is critical for the survival of both RPE and photoreceptors.

#### KEYWORDS

CLC-2, photoreceptor degeneration, RPE, subretinal space

## 1 | INTRODUCTION

The retinal pigment epithelium (RPE) and photoreceptors are highly polarized cells, which establish a functional unit in the outer retina. While these cells differentiate simultaneously in the first trimester of human pregnancy, they develop postnatally in rodents.<sup>1,2</sup> During this developmental stage, long microvilli extend from the apical surface of the RPE and wrap around the photoreceptor outer segments, a process controlled by ezrin.<sup>3</sup> There is clear evidence that functional and properly polarized RPE cells are essential for the morphogenesis, function and, survival of photoreceptors.<sup>4-7</sup> The support function of RPE for photoreceptors and the neural retina is mediated by the ability of RPE cells to vectorially secrete growth factors asymmetrically such as apical PDGF<sup>8</sup> and basolateral VEGF, to perform daily phagocytosis of photoreceptor outer segments,<sup>9</sup> to participate in the regeneration of visual pigments and to act as the major blood-retinal barrier between the subretinal space and the underlying choroidal blood vessels.<sup>2,10,11</sup> This barrier role of RPE is dependent on the establishment of functional tight junctions between the apical poles of neighboring cells<sup>12</sup> and on the polarized distribution of ion channels and transporters between apical and basolateral plasma membrane domains.<sup>2,13</sup> In turn, this asymmetry is essential for the vectorial transport of electrolytes, glucose, amino acids, and other nutrients from the choroidal vasculature to the subretinal space and fluid and photoreceptor metabolic byproducts in the opposite direction.<sup>2</sup> Deficiencies in the function or polarity of RPE transporters may cause defects in photoreceptor morphogenesis resulting in retinal degeneration and blindness.<sup>1,2,14</sup>

The metabolic activity of photoreceptors and the neural retina generate large amounts of water and lactate requiring the transport activities of RPE cells to regulate the composition and pH of the subretinal space; this is essential for the function and survival of photoreceptors. Transport of water by the RPE generates a negative pressure in the subretinal space that is necessary for RPE adhesion to the neural retina.<sup>2,10</sup> Transport of fluid is secondary to ion transport processes. The apical Na<sup>+</sup>/K-ATPase pumps Na<sup>+</sup> toward the subretinal space generating

a Na<sup>+</sup>-gradient that facilitates the entrance of Cl<sup>-</sup> and K<sup>+</sup> by a bumetanide-sensitive (NKCC) cotransporter in the apical plasma membrane.<sup>15-18</sup> Intracellular Cl<sup>-</sup> and Na<sup>+</sup> concentrations are also regulated by bicarbonate exchangers which, together with lactate transporters MCT1 and MCT3, regulate subretinal and intracellular pH.<sup>2</sup> Accumulation of Cl<sup>-</sup> results in a high intracellular concentration of ~60 mM that, coupled to the favorable trans-membrane electric potential across the basolateral PM, promotes exit of Cl<sup>-</sup> toward the choroidal space, with K<sup>+</sup> as a counter-ion.<sup>19</sup> Transporters mediating K<sup>+</sup> and Cl<sup>-</sup> exit toward the choroid remain poorly characterized.

One of the candidates to perform this function is chloride channel protein 2 (CLCN2 aka CLC-2). CLC-2 is a ubiquitous voltage-gated chloride channel, particularly abundant in epithelial tissues,<sup>20-22</sup> which is believed to mediate trans-epithelial Cl<sup>-</sup> transport processes at the basolateral membrane of intestinal cells in response to cell swelling and extracellular acidification.<sup>23,24</sup> The knockout of CLC-2 in mice causes blindness by retinal degeneration and male sterility.<sup>25,26</sup> These findings are consistent with its expression in blood-tissue epithelial barriers, that is, RPE in retina and Sertoli cells in testis.<sup>2,24,25</sup> In epithelial cells from rat or mouse colon and small intestines, CLC-2 has been shown to localize to the lateral plasma membrane.<sup>23,26</sup> Our laboratory has shown that, in the polarized kidney epithelial cell line MDCK, CLC-2 localizes basolaterally, which is mediated by the clathrin adaptor AP-1.<sup>27</sup> Based on physiological experiments, CLC-2 has been suggested to function on the basolateral membrane of RPE cells, where it would contribute to vectorial fluid transport from the subretinal space to the underlying choroid.<sup>2,28</sup> However, this localization has not been studied by immunolocalization techniques, because of the lack of appropriate CLC-2 antibodies.

In this report, we show that tissue-specific reconstitution of CLC-2 into the RPE of CLC-2 KO mice prevents RPE and photoreceptor cell death. Surprisingly, we identified the restricted localization of CLC-2 protein to the apical plasma membrane in the mouse RPE monolayer. Our results suggest a key role of CLC-2 in regulating the subretinal environment of RPE and photoreceptors that is vital for the maintenance and survival of both cell types.

## 2 | MATERIALS AND METHODS

### 2.1 | Generation of CLC-2 knockout mice and PCR genotyping

CLC-2-deficient mice were kindly provided by James Melvin.<sup>29,30</sup> Homozygous knockouts were viable and developed normally as previously described.<sup>25,26,29,30</sup> For our study, heterozygous knockouts were crossed to obtain homozygous mutant mice, as well as heterozygous knockout and wild type mice as control animals. We confirmed the correct deletion of *CLC-2* by PCR genotyping strategy to distinguish between wild type, heterozygous and homozygous knockouts. Genomic DNA was isolated from mouse tails using Qiagen Kit (#69506) and genotyping PCR was performed using the following 5'-end-primer set: Neo-KO-F: CCTGGAAGGTGCCACTCCCACTGTCC; CLC-2-KO-F: ATGTATGGCCGGTACACTGAGGGACTC; CLC-2-KO-R: ACACCCAGGTCCCTGCCCAATCTGG. PCR yields an amplicon of 190 bp for wild type allele and 300 bp for mutant allele. We confirmed the lack of *rd1* and *rd8* mutations as previously described.<sup>31,32</sup> To visualize the photoreceptor primary cilium, we cross-bred *CLC-2*<sup>-/-</sup> mice with transgenic *Centrin2*<sup>GFP</sup> (*Cem2*<sup>GFP</sup>) and *Arl13b*<sup>mCherry</sup> (*Arl13b*<sup>mCh</sup>) (JAX, 027967) labeling centrioles/transition zone and the outer segment, respectively. Mouse work was performed in accordance with procedures approved by the Institutional Animal Care and Use Committees of Weill Cornell Medical College (registry #2010-0086). Mice were kept under a 12/12-h light/dark cycle.

### 2.2 | Antibodies

The following primary antibodies were used: mouse anti-HA (1:500, MMS-101P, Covance, Princeton, NJ); rabbit anti-MCT1 YZ4715 (0.86 mg/mL; 1:500); rabbit anti-ZO-1 (1:500; Invitrogen, 61-7300); mouse anti-GP135 (1:500, Sigma, MABS1327); mouse anti-ezrin (1:250; 3C12 Sigma, E08897); CF488A-conjugated anti-Phalloidin (1:250; Biotium, 00042). Bound primary antibodies were visualized with appropriate secondary antibodies conjugated with Alexa Fluor 488, 568 or 647 (1:1000; Invitrogen, Life Technologies) and nuclei were stained with 10 µg/mL Hoechst (Thermo Fisher Scientific, H3569).

### 2.3 | Retinal cross-sections and immunofluorescence

Retinal cross-sections were prepared as previously described.<sup>33,34</sup> Mouse eyecups were placed in 4% paraformaldehyde in PBS for 2 hours at room temperature (RT). After

fixation, eyecups were rinsed in PBS and embedded in 7% low-melt agarose (A3038; Sigma Aldrich). The agarose-embedded eyecups were Vibratome sectioned into 100 µm-thick slices (VT1200S; Leica), which were then blocked in PBS containing 5% goat serum and 0.5% Triton X-100 for 1 hour at RT. The sections were incubated with primary antibodies overnight at 4°C, washed three times in PBS for 10 minutes each, and incubated for 2 hours at RT with appropriate secondary antibodies. Stained slices were washed three times in PBS for 10 minutes each, mounted onto slides in Fluoromount G (Electron Microscopy Sciences) and coverslipped. Images were taken with a confocal microscope (Eclipse 90i and A1 confocal scanner; Nikon) with a 60× objective (1.4 NA Plan Apochromat VC; Nikon) using Nikon NIS-Elements software. Image analysis and processing was performed with ImageJ and Nikon NIS-Elements software.

### 2.4 | RPE flat mounts

RPE flat mounts were obtained by detaching the retina from the whole mounts, which were fixed and immunostained as retinal cross-sections (see above). To avoid artefactual removal of the primary cilium, microvilli, and apical membrane of the RPE through peeling of the neural retina, mice were dark adapted overnight. For imaging, the RPE was placed up, facing the coverglass, when mounted on slides. Images were taken with a Zeiss Cell Observer SD confocal with a Yokagawa CSU-X1 spinning disk, using a Plan-Apochromat 20×/0.8 air objective or 63×/1.4 M27 oil-immersion objective. Images were generated using either Zeiss software Zen2.6 (Carl Zeiss Micro Imaging, LLC, Thornwood, NJ) or ImageJ.

### 2.5 | Histology and transmission electron microscopy

Mice were deeply anesthetized transcardially perfused with 2% paraformaldehyde and 2% glutaraldehyde in 0.05% calcium chloride in 50 mM MOPS (pH 7.4).<sup>35</sup> The eyes were enucleated and fixed for an additional 2 hours in the same buffer at RT. For thin plastic retinal sections, eyecups were cut in half through the optic nerve and embedded in Spurr's resin (Electron Microscopy Sciences). For light microscopy, 500 nm thin retinal cross sections were cut and stained with methylene blue, as described in.<sup>34,36</sup> For electron microscopy, 70 nm thin sections were cut, placed on copper grids, and counterstained with 2% uranyl acetate and 3.5% lead citrate (19314; Ted Pella). The samples were imaged on a JEM-1400 electron microscope (JEOL) with a digital camera (Orius, Gatan).

## 2.6 | Lentivirus generation and transduction

Wild type form of CLC-2-HA<sup>27</sup> was cloned into *AgeI* and *Sall* restriction sites of pCCL-PGK-GFP lentiviral vector (pRRLSIN.cPPT.PGK-GFP.WPRE; Addgene; Plasmid #12252) replacing GFP, and then human Best1 promoter (−588 to +58)<sup>37</sup> was cloned into *XhoI* and *AgeI* replacing PGK promoter. Lentivirus was generated as previously described.<sup>27,38</sup> Briefly, 3x10<sup>6</sup> HEK293T cells in DMEM with 10% FBS were transfected with third generation lentivirus (10 µg viral backbone, 3 µg VSV-G, 5 µg RRE, and 2.5 µg REV) and viral supernatant was concentrated 100-fold with Lenti-X Concentrator (Clontech #631231) following the manufacturer's instructions. A viral titer of 14 × 10<sup>6</sup> RNA copies/µL of concentrated lentivirus was determined and aliquots were stored at −80°C for immediate use. For *CLC-2<sup>-/-</sup>* rescue study, lentivirus was subretinally injected shortly after eye opening as previously described in<sup>39</sup> and eyes were harvested at 6-8 weeks post-injection for imaging.

## 2.7 | Electroretinogram

Animals were dark-adapted overnight, and anesthesia was subsequently delivered in the amount of ~20/2 mg/kg ketamine/xylazine solution per hour. Anesthetized animals were placed on a stage with a heater to keep the appropriate body temperature. The pupils were then dilated with one drop per eye of 1% Cyclopentolate/2.5% Phenylephrine solution and one drop of Gonak (Akorn) applied along with careful placement of the gold wire corneal electrodes. Light flashes or constant illumination of various durations and intensities were delivered to the anesthetized animals to evoke ERGs (Ganzfeld ColorDome Diagnosis LLC). For scotopic ERGs, single-flash scotopic responses were recorded at various stimulus intensities of −6.91 log cds·m<sup>−2</sup> to 3.00 log cds·m<sup>−2</sup>. For photopic ERGs, the mice were light-adapted under background light of 1.48 log cds·m<sup>−2</sup> for approximately 5-10 minutes. Single-flash photopic responses were recorded at stimulus intensities of 0.00 log cds·m<sup>−2</sup> to 3.40 log cds·m<sup>−2</sup>. In these experiments both eyes were subject of light conditioning ERG recordings simultaneously. Recorded ERG traces were analyzed with *software* Diagnosis Espion and Prism.

## 3 | RESULTS

### 3.1 | Loss of CLC-2 causes fast progression of retinal degeneration

Previous studies reported that in *CLC-2* KO mice photoreceptors degenerate rapidly after eye opening and mice are

blind in early adulthood.<sup>25,29,30</sup> To document the alterations in retinal structure caused by absence of *CLC-2*, we analyzed retinal cross-sections from heterozygous controls (*CLC-2<sup>+/-</sup>*) and homozygous knockout animals (*CLC-2<sup>-/-</sup>*) at P2, P7, P14 and one month (1M) of age (Figure 1A,B). In knockout (*CLC-2<sup>-/-</sup>*) mice, photoreceptors start to degenerate between P7 and P14, and the degeneration is complete by 1M of age, with nearly complete loss of outer segments, inner segments, and only sparse remnants of the outer nuclear layer by 1M, indicating that *CLC-2* is important for retinal structure and photoreceptor survival.

Interestingly, ultrastructural analysis of the outer segments in mutant *CLC-2<sup>-/-</sup>* mice (Figure 1C,D) show that, at P14, disc membranes are formed at the base of the developing rods and cones, allowing them to moderately see at early age, albeit they have a loss of vision by 1M.<sup>26</sup> Therefore, we conclude that *CLC-2* is not required for early photoreceptor development, in particular photoreceptor ciliogenesis and the formation of the nascent outer segment. However, distal outer segment discs appear severely disorganized and malformed at P14, which is two days after eye-opening, and disc-like structures almost completely disappear at 1M of age (Figure 1D). In contrast, in *CLC-2<sup>+/-</sup>* mice, outer segments develop normally, and discs are well organized (Figure 1C). Parallel experiments (data not shown) show that retinal degeneration is only observed in homozygote (*CLC-2<sup>-/-</sup>*), but not in heterozygote (*CLC-2<sup>+/-</sup>*) and wild type mice. Hence, for the experiments presented in this manuscript, we used *CLC-2<sup>+/-</sup>* mice as controls.

### 3.2 | RPE loss in *CLC-2* knockout mice

It has been proposed that the fast-progressing retinal degeneration of the photoreceptors is secondarily caused by a change in the mouse RPE monolayer.<sup>25,26,30,40</sup> Therefore, we investigated the post-natal development of the apical pole of RPE cells in *CLC-2<sup>+/-</sup>* and *CLC-2<sup>-/-</sup>* mice by localizing in RPE flat mounts the tight-junction marker ZO-1 (Figure 2A-D) and the microvilli marker F-actin (Figure 2E-H) at different ages. At P2, tight-junctions and microvilli staining were comparable in both genotypes (Figure 2A,E). At P7, microvilli appeared undeveloped and disrupted in *CLC-2* deficient mice, relative to control mice (Figure 2H), whereas tight-junctions are intact in both (Figure 2B). We observed more severe alterations of the apical pole of RPE cells starting at P14. In particular, ZO-1 was found in small intracellular vesicles at P14 (Figure 2C, right panel, arrowheads) and accumulated at branch points at 1M of age (Figure 2D, right panel, asterisks). In addition, F-actin-labelled microvilli appear highly disorganized or absent in homozygous knockouts at P14 and 1M of age (Figure 2G,H). Together, our data suggest a functional role of *CLC-2* in the postnatal development and maintenance of the apical pole of mouse RPE cells.

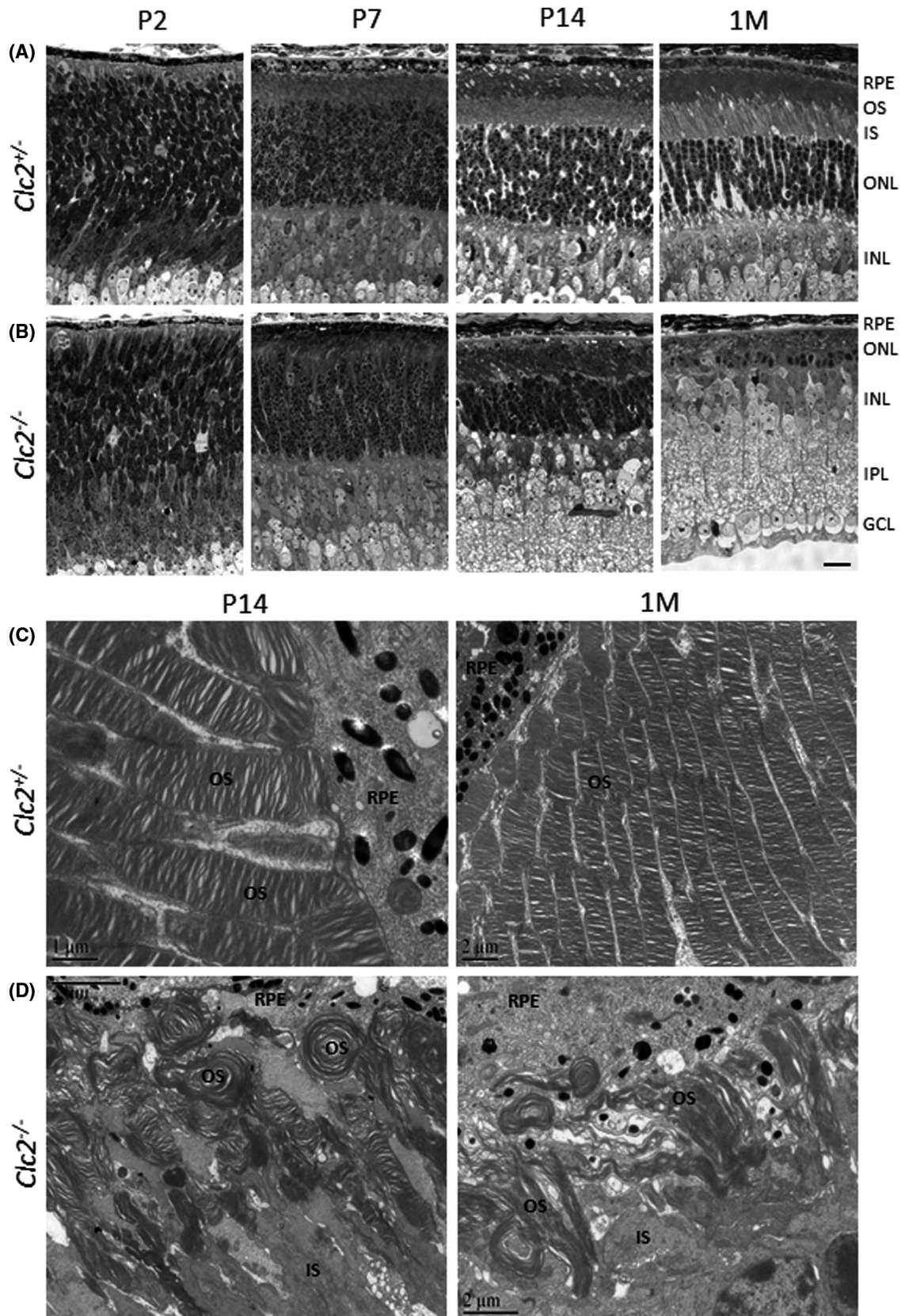


**FIGURE 1** Loss of CLC-2 causes fast progress of retinal degeneration. A,B, Retinal cross-sections from tissue of *CLC-2*<sup>+/+</sup> (A) and *CLC-2*<sup>-/-</sup> mice (B) were processed for optical microscopy at P2, P7, P14, and 1M of age. The early loss of photoreceptors is reflected by progressive thinning of the outer nuclear layer (ONL) between P7 and P14 and the degeneration is complete at 1M of age. Scale bar: 20 μm. C,D, Electron microscopic analysis of the photoreceptors in *CLC-2*<sup>-/-</sup> mice shows that outer segments (OS) are formed, however distal OS discs are severely disorganized at P14 and 1M of age (D) in comparison to well-structured OS in control mice (C)

### 3.3 | Localization of the apical RPE marker MCT1 is disrupted in CLC-2 knockout mice

To further investigate changes in the apical pole of RPE cells in CLC-2 knockout mice, we examined the distribution of the apical marker, monocarboxylate transporter 1 (MCT1) in retinal cross-sections and RPE flat mounts obtained from *CLC-2<sup>+/-</sup>* and *CLC-2<sup>-/-</sup>* mice at P7, P14 and 1M of age (Figure 3). In retinal cross-sections from P7 and P14 control mice, MCT1 staining appeared as a thin band, corresponding to nascent RPE microvilli, directly opposed to developing photoreceptor outer segments stained with the ciliary marker *Arl13b<sup>mCh</sup>* (Figure 3A,B). In 1M-old mice, the MCT1 band appeared thicker, consistent with the existence of mature, apical microvilli at this time (Figure 3C). In homozygous CLC-2 knockouts, a relatively normal thickness of photoreceptor outer segment layer was observed at P7, whereas MCT1 staining appeared thinner than in control cells (Figure 3D), in agreement with the decreased staining of microvilli actin-staining of microvilli observed at this age (Figure 2). In P14 and 1M-old retinas, the layer of photoreceptor outer segments had rapidly degenerated (P14) and practically disappeared (1M):

at these times the band of MCT1 staining was much thinner than in control retinas (Figure 3E,F). In en face views of RPE flat mounts, MCT1 appeared quite homogeneously distributed in the apical pole of control *CLC-2<sup>+/-</sup>* mice at P7 (with cell outlines visible), more homogeneously distributed at P14 (with cell outlines lost) and diffusely distributed at 1M of age, with some disruptions probably caused by the mechanical removal of the RPE monolayer during preparation of the flat mount at a time when adhesion between RPE and neural retina is maximal (Figure 3G). In contrast, MCT1-staining in *CLC-2<sup>-/-</sup>* mice appeared progressively disrupted (Figure 3H); additional co-staining of RPE flat mounts with the apical marker GP135 (*aka* podocalyxin) confirmed the disruption of the apical membrane surface at P7 and 1M of age (Supplemental Figure S1). Parallel co-staining of the apical microvilli marker ezrin demonstrated a similar disruption of its apical localization as observed for MCT1 in the developing retina (Figure 3I,J). Taken together, the phenotypic characterization of CLC-2 knockout mice in early adulthood is consistent with a developmental disruption of the apical pole of RPE cells (Figures 2 and 3) that correlates in time with a rapid degeneration of the photoreceptors (Figure 1).

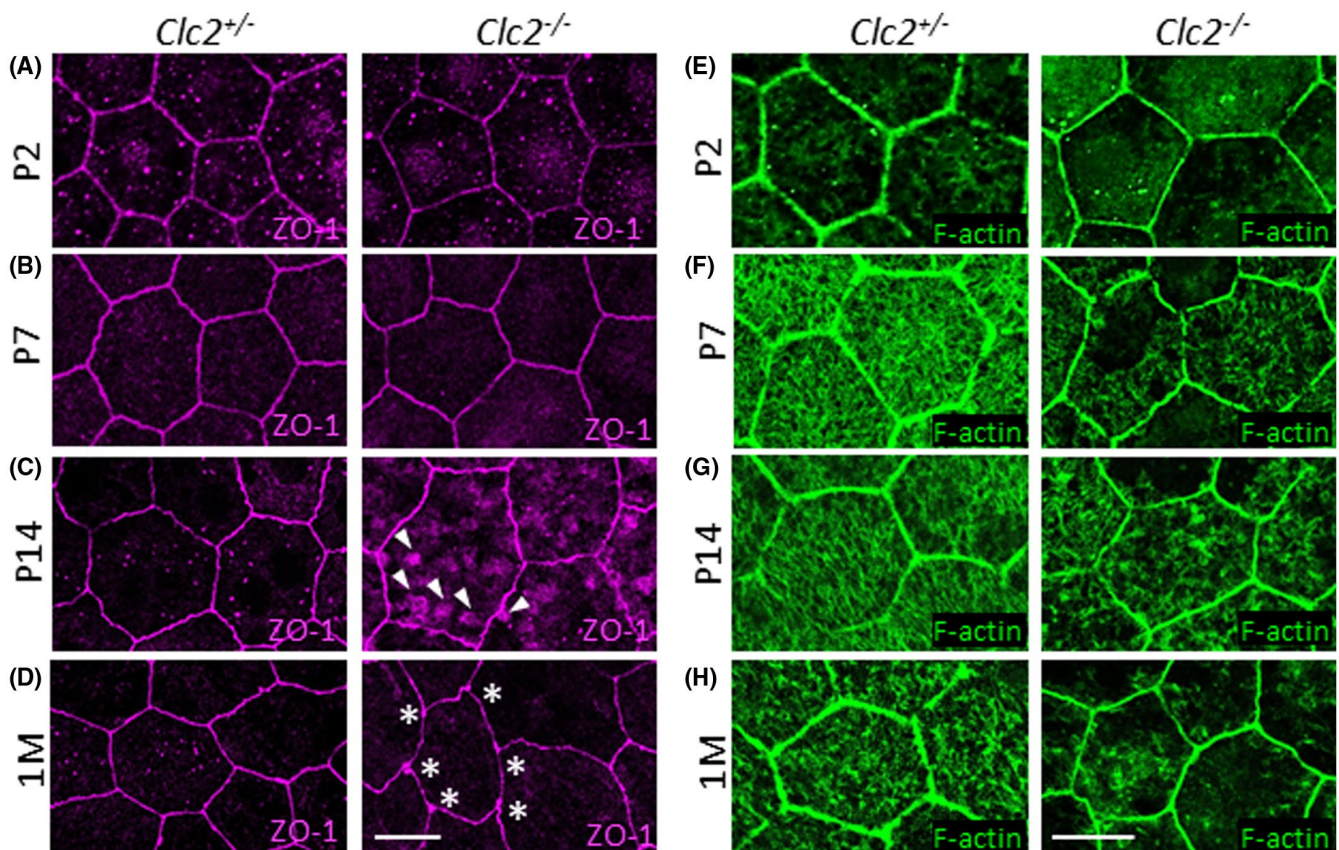


**FIGURE 2** RPE loss in CLC-2 knockout mice. RPE flat mounts from heterozygous (left panels) and homozygous (right panels) knockout animals were stained with tight-junction marker ZO-1 (A-D) and microvilli marker F-actin (E-H) at P2, P7, P14, and 1M of age. In absence of CLC-2, ZO-1 concentrates in intracellular vesicles at P14 (E, right panel, arrow heads) and accumulates at RPE branch points at one month (F, right panel, asterisks). F-actin-labelled microvilli appear disrupted as early as P7 (F-H, right panels). Scale bar: 10  $\mu$ m

### 3.4 | Ultrastructural analysis of the disrupted interaction between RPE and photoreceptors in the *CLC-2*<sup>-/-</sup> retina

In order to characterize at higher resolution, the disruption of the apical pole of RPE cells and photoreceptor outer segments, we performed ultrastructural analysis of this interaction at P14 (Figure 4). Control heterozygous *CLC-2*<sup>+/-</sup> retinas displayed elongated RPE microvilli surrounding photoreceptor outer segments loaded with parallel discs and melanosomes localized on the apical half of the RPE cytoplasm (Figure 4A-C). In contrast, homozygous knockouts displayed RPE cells with highly disrupted microvilli and melanosomes all over the cytoplasm; neighboring photoreceptors were malformed with the distal tips lacking well organized discs (Figure 4D-H). Furthermore, the basal infoldings and the underlying Bruch's membrane also presented as less developed and malformed (Figure 4D-H). The very disorganized appearance of the apical pole of RPE cells and photoreceptor tips suggests that the normal interaction between these two cells is highly disrupted, which is consistent with a role of CLC-2 in the maintenance of a normal subretinal space, necessary for the correct morphogenesis and survival of these two retinal cells.

### 3.5 | RPE-specific expression with hBest1<sub>promoter</sub>CLC-2-HA in *CLC-2* knockouts

To investigate whether the retinal degeneration is indeed caused by the deletion of CLC-2 in the RPE monolayer, we generated lentivirus expressing CLC-2 tagged with hemagglutinin (HA) under the control of the RPE-specific promoter human-bestrophin1 (hBest1<sub>promoter</sub>) and delivered the virus via subretinal injections in *CLC-2*<sup>+/-</sup> and *CLC-2*<sup>-/-</sup> mice shortly after eye-opening. Bestrophin-1 is an RPE-specific Ca<sup>++</sup>-activated Cl<sup>-</sup> channel.<sup>41</sup> Expression of CLC-2 under these conditions was restricted to RPE cells.<sup>37</sup> At 6-8 weeks post-injection, we collected RPE flat mounts and analyzed the expression of HA-tagged CLC-2 protein (CLC-2-HA) in lentivirus-transduced (*LV*<sup>+</sup>) heterozygous controls and homozygous knockouts (Figure 5A-D). We found that CLC-2-HA is expressed in ~60 to 70% of RPE cells throughout the entire RPE flat mounts (Figure 5C,D) and is absent in untransduced control animals (Figure 5A,B).

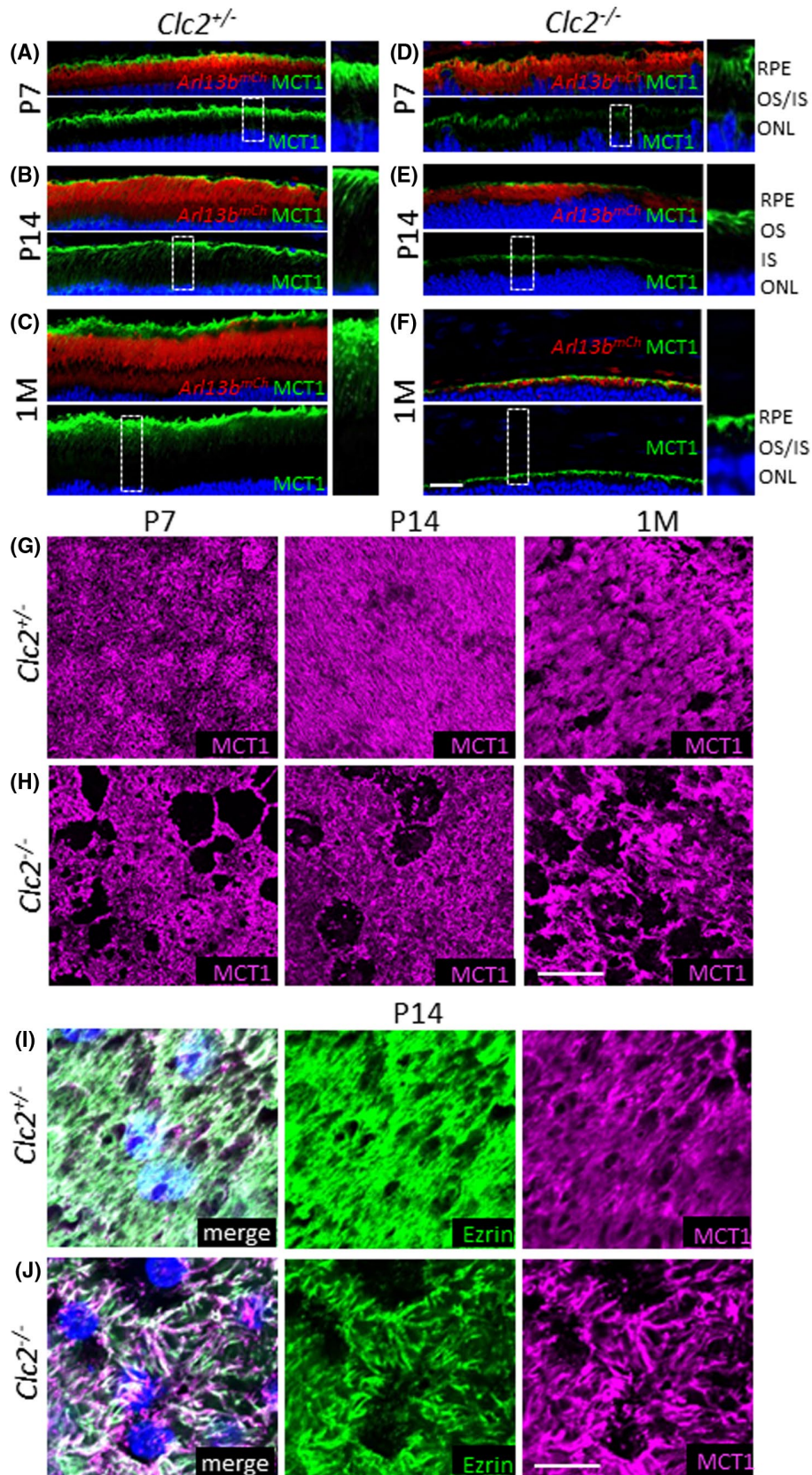
To examine the localization of CLC-2 in RPE cells, cross-sections of *CLC-2*<sup>+/-</sup> retinas transduced with CLC-2-HA were decorated for immunofluorescence with anti-HA (Figure 5E) and anti-MCT1 (Figure 5F) antibodies. Strikingly, CLC-2 localization (Figure 5E) was matched that observed for the apical RPE marker MCT1 (Figure 5F), suggesting that CLC-2-HA is restricted to the apical surface of RPE cells. This result is unexpected as physiological data has suggested that

CLC-2 participates in the transport of Cl<sup>-</sup> at the basolateral membrane.<sup>2</sup> The apical localization of CLC-2 strongly suggests an important role of CLC-2 in the homeostasis of the subretinal space, necessary for developmental morphogenesis and survival of RPE, and photoreceptors.

### 3.6 | Expression of CLC-2-HA in RPE cells prevents photoreceptor degeneration and rescues the normal distribution and morphology of apical MCT1 in RPE cells

We analyzed the retinal histology of lentivirus-transduced eyes to test whether the RPE-specific expression of CLC-2-HA rescues photoreceptor degeneration in *CLC-2*<sup>-/-</sup> mice (Figure 6). Plastic sections of untransduced heterozygote (*CLC-2*<sup>+/-</sup>), untransduced homozygote (*CLC-2*<sup>-/-</sup>), and transduced homozygote (*Clc2*<sup>-/-</sup>; *CLC-2-HA LV*<sup>+</sup>) were stained with methylene blue and analyzed by regular histology. Control (*CLC-2*<sup>+/-</sup>) retinas displayed the normal structure of the retina with 10-12 nuclear layers in ONL and normal photoreceptor inner and outer segments (Figure 6A). In contrast, KO (*CLC-2*<sup>-/-</sup>) mice completely lacked ONL and photoreceptor outer/inner segments (Figure 6B). Strikingly, KO (*CLC-2*<sup>-/-</sup>) retinas transduced with CLC-2-HA displayed more normal photoreceptors, with ONL consisting of 4-6 nuclear layers and well developed, albeit shorter, outer/inner segments (Figure 6C). From the number of nuclear layers recovered it may be estimated that 50-60% of the photoreceptors were rescued. Transduction with empty lentivirus did not prevent the degeneration of the photoreceptors and lack ONL and photoreceptor outer/inner segments as seen in untransduced homozygote animals (Supplemental Figure S2). This rescue experiment strongly suggests that the loss of photoreceptors in *CLC-2*<sup>-/-</sup> mice is primarily caused by an alteration in the RPE function caused by the absence of CLC-2.

To characterize the recovery of rescued CLC-2 KO eyes, we analyzed the RPE morphology and the localization of the apical marker MCT1. To this end, the hBest1<sub>promoter</sub>CLC-2-HA transduced (at P14) heterozygous and homozygous knockout mice, aged to 2M, were used to prepare RPE flat mounts by mechanical detachment from neural retinas and co-labelled them with anti-MCT1 and anti-HA antibodies (Figure 6D-I). In presence of endogenous CLC-2, MCT1 displays a normal localization with a diffuse apical staining pattern, consistent with long and well-developed microvilli (Figure 6D: xz-view and G). In *CLC-2* KO mice aged 2M, MCT1 has a very altered distribution pattern, with little MCT1 protein displaying an apical staining pattern (Figure 6E: xz-view and H). Remarkably, the expression of exogenous CLC-2 protein in



*CLC-2*<sup>-/-</sup> mice restores an apical staining pattern of MCT1 (Figure 6F: xz-view and I, lower panel), similar to that observed for untransduced heterozygous controls (Figure 6G,

lower panel). Interestingly, individual RPE cells show various expression levels of CLC-2-HA with some of them lacking CLC-2: however all RPE cells recover apical staining pattern

**FIGURE 3** Apical localization of MCT1 is disrupted in *CLC-2* knockout mice. A-F, Retinal cross-section from *CLC-2*<sup>+/-</sup>; *Arl13b*<sup>mCh</sup> (A, B and C) and *CLC-2*<sup>-/-</sup>; *Arl13b*<sup>mCh</sup> (D, E and F) mice were labelled with anti-MCT1 antibody (green) at P7, P14 and 1M of age. The transgenic expression of ARL13b-mCherry (*Arl13b*<sup>mCh</sup>) labels the photoreceptor primary cilium. The disruption of the apical localization of MCT1 (green, enlargements) in homozygous knockouts causes OS shortening at P7 (D) and the photoreceptors degenerate rapidly between P14 (E) and one month (F). In contrast, MCT1 is strongly expressed in apical RPE microvilli in *CLC-2*<sup>+/-</sup>; *Arl13b*<sup>mCh</sup> mice (D-F): MCT1 appears as a thin band at P7 (A) and largely localizes to apical RPE microvilli at P14 (B) and 1M of age (C). Scale bar: 20  $\mu$ m. G-J, RPE flat mounts from *CLC-2*<sup>+/-</sup> (G and I) and *CLC-2*<sup>-/-</sup> (H and J) mice were labelled with microvilli markers MCT1 (G-J) and ezrin (I and J) at P7, P14, and 1M of age. The loss of *CLC-2* disrupts the apical localization of MCT1 in RPE cells (H) and parallel staining with ezrin confirms the disruption of the apical membrane surface (J) compared to controls. Scale bar: 20  $\mu$ m G-H; 5  $\mu$ m I-J

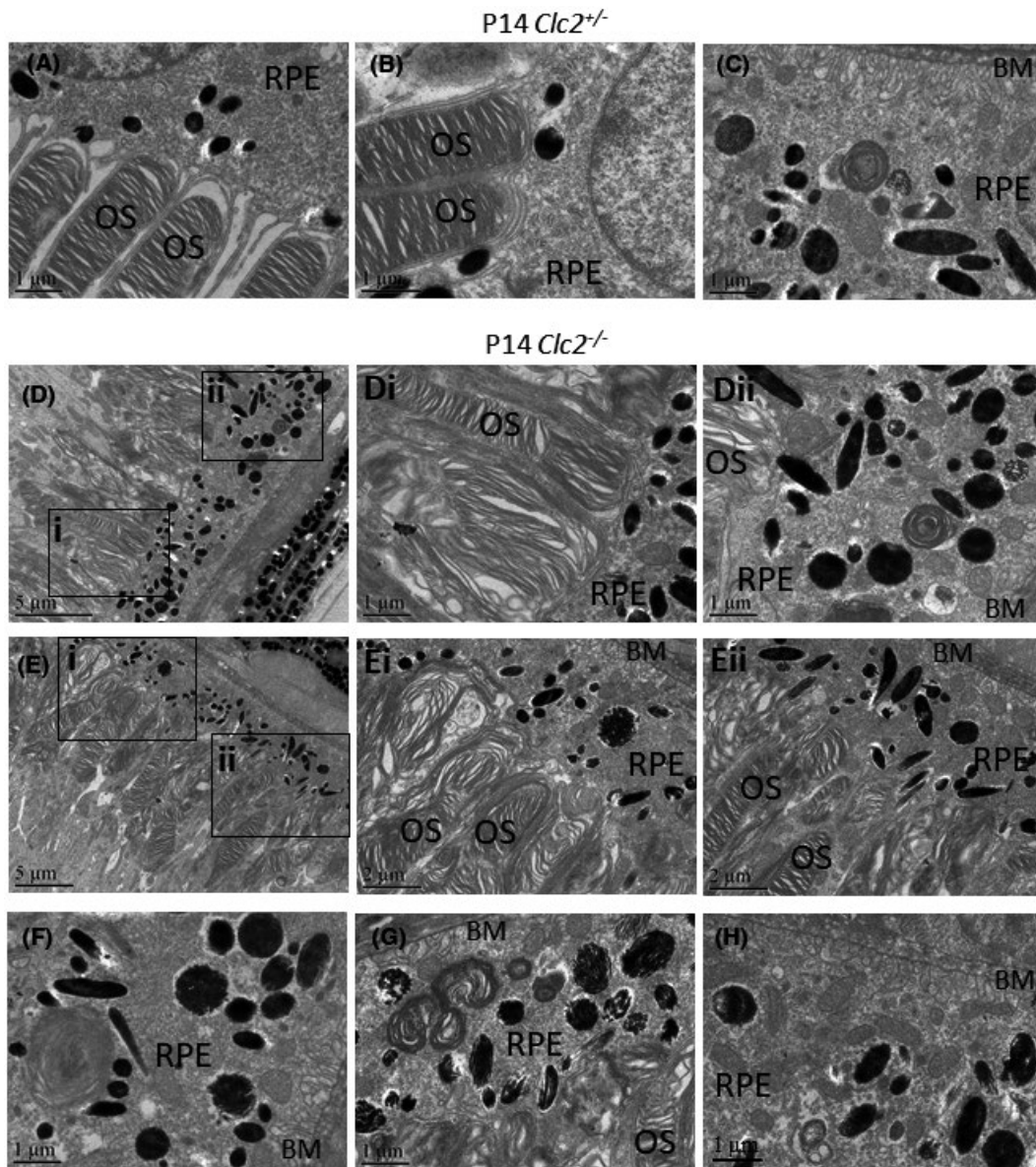


**FIGURE 4** Ultrastructural analysis of *CLC-2* knockout retinas. The connection between the photoreceptors and the RPE monolayer was analyzed at ultrastructural level at P14. In *CLC-2*<sup>+/-</sup> retinas (A-C), OS are well-organized, microvilli surround the distal disc membranes and RPE, including the Bruch's membrane (BM) and melanosomes, appear normal. *CLC-2*<sup>-/-</sup> photoreceptors are normally-stacked near the inner segment (D and E), however become largely disorganized distally with membrane material accumulating more disorderly close to the RPE (Di, Ei and Eii). In *CLC-2*<sup>-/-</sup> RPE cells, microvilli are disrupted, basal infoldings are less pronounced, and the BM appears thinner and melanosomes are all over the cytoplasm (Dii, F-H)

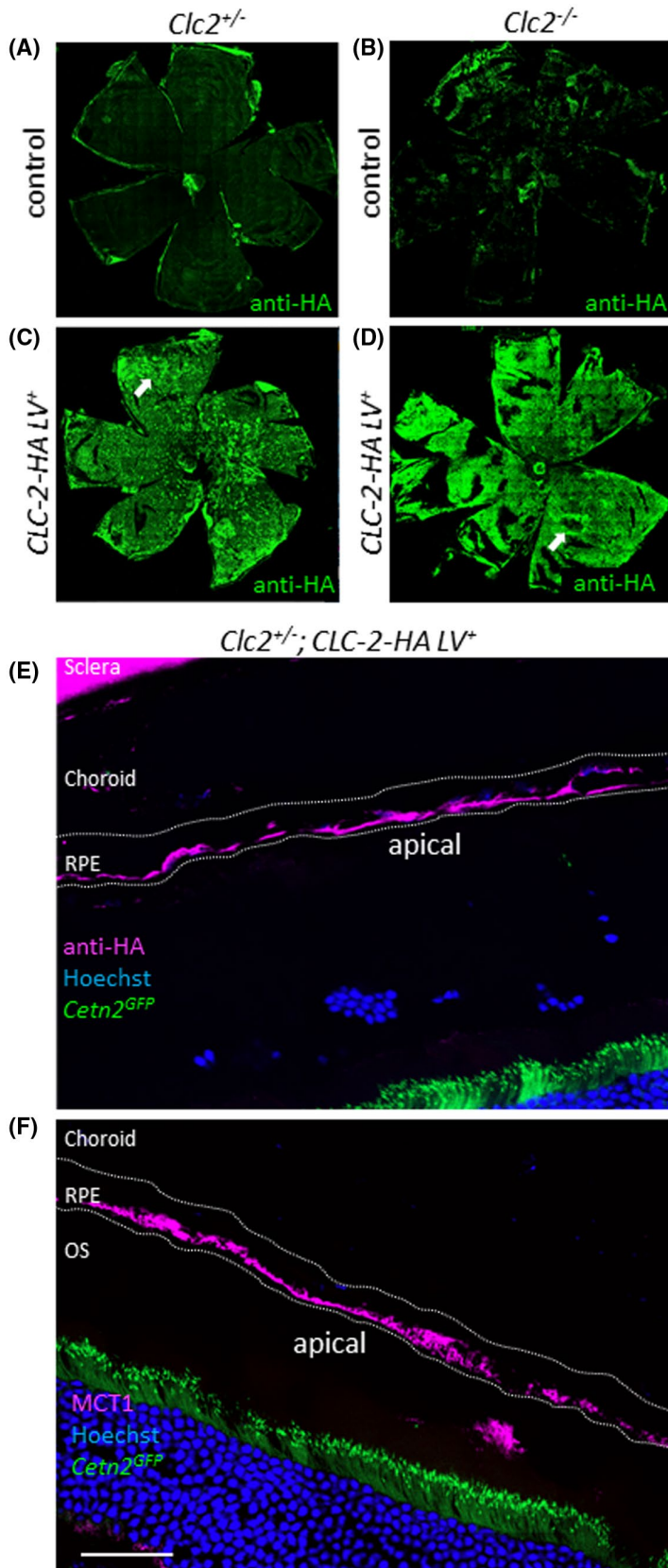


**FIGURE 5** Lentiviral expression of hBest1<sub>promoter</sub>CLC-2-HA. A-D, RPE flat mounts from untransduced (control) and lentivirus (LV)-injected eyes (LV<sup>+</sup>) were labelled with anti-HA antibody (A-D). *CLC-2*<sup>+/-</sup> (A and C) and *CLC-2*<sup>-/-</sup> RPE flat mounts (B and D) show expression of hBest1<sub>promoter</sub>CLC-2-HA (green) in transduced eyes (C and D, white arrows indicate injection side), whereas HA-specific staining is absent in untransduced controls (A and B). Scale bar: 500 μm. E-F, Retinal cross-sections from LV-injected retinas (E and F) show specific localization of hBest1<sub>promoter</sub>CLC-2-HA (E) on the apical pole of RPE cells, a similar localization pattern as the apical membrane protein MCT1 (F). Transgenic expression of *Cetrn2*<sup>GFP</sup> visualizes the photoreceptor transition zone, which is used as reference for orientation in the outer retina. Scale bar: 20 μm

of MCT1 (Figure 6I). The more clearly delineated cell shapes observed for MCT1-stained, recovered RPE cells probably corresponds to the expression of shorter microvilli in these cells relative to control heterozygote cells (see Figure 3G).

Next, we characterized functionally the rescued *CLC-2* KO eyes by electroretinography (Figure 7). Scotopic and photopic ERG in control heterozygote retinas detected characteristic A- and B-waves under dark and daylight conditions (Figure 7A,D)

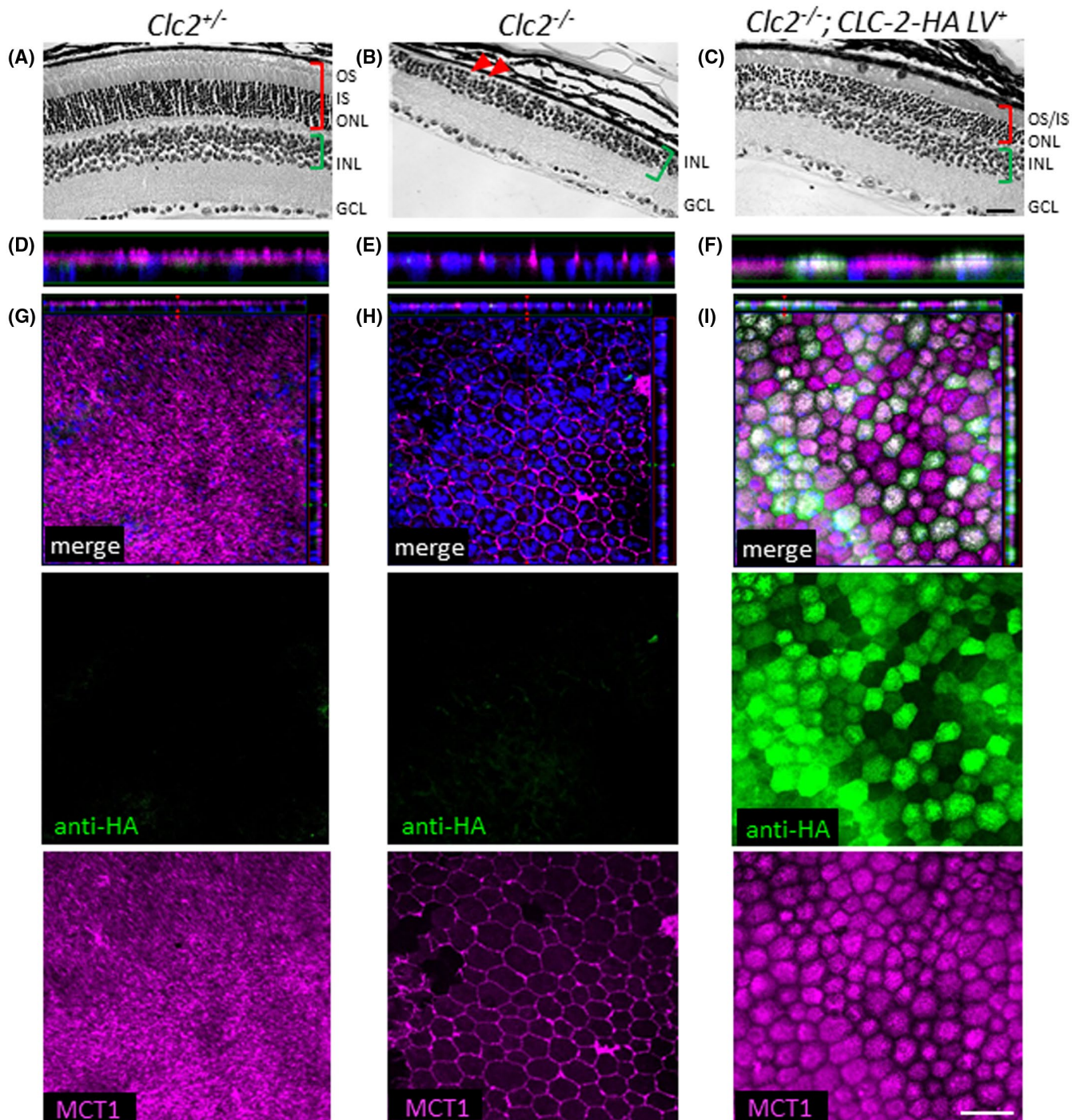


**FIGURE 6** hBest1<sub>promoter</sub>CLC-2-HA reduces the severity of photoreceptor degeneration and rescues apical localization of MCT1. Retinal cross-sections from untransduced heterozygous control (A) and untransduced homozygous knockouts (B) show 10-12 nuclei layers in the ONL are present in control retinas (A, red indicates photoreceptor layer and green the inner nuclear layer) versus the ONL in *CLC-2*<sup>-/-</sup> mice is degenerated (B, red arrows indicate single photoreceptor nuclei and green the INL). In untransduced RPE flat mounts, MCT1 shows apical staining-pattern in *CLC-2*<sup>+/-</sup> mice (D: xz-view and G), whereas it is largely disrupted in *CLC-2*<sup>-/-</sup> mice (E: xz-view and H). Lentivirus was subretinally injected at eye opening (P12) in knockout animals and tissue was harvested at 2M of age. The expression of CLC-2 under the control of RPE-specific Bestrophin-1 promoter (hBest1<sub>promoter</sub>) rescues the retinal degeneration and sustained photoreceptors in mutant mice (C, thickness of the photoreceptor layer, including the OS, is highlighted in red); n = 3. Remarkably, the treatment with LV-expressing CLC-2 protein in homozygous knockouts rescues the apical MCT1 staining-pattern in RPE cells (F: xz-view and I: lower panel), resembling the distribution pattern of CLC-2-HA at the apical membrane surface (I, middle panel); n = 3. Scale bar: 20 μm

and a loss of practically all electric activity with a subtle response to light at the brightest stimulation in homozygote KO mice (Figure 7B,E). In contrast, CLC-2 transduced homozygote KO mice display distinctive scotopic and photopic ERG traces with all but the dimmest light stimuli, an improvement from the untransduced  $CLC-2^{-/-}$  mice (Figure 7C,F). The scotopic A-wave in transduced eyes is approximately equal in amplitude to the photopic amplitudes (Figure 7C,F), while wild type mice typically have scotopic A-waves nearly tenfold greater with bright light stimulation (Figure 7A), indicating only a partial restoration of vision. To conclude, the RPE-specific re-expression of CLC-2 partially restores RPE and photoreceptor morphology, allowing mutant mice to maintain a distinct but reduced level of visual function after rescue.

## 4 | DISCUSSION

Previous work has demonstrated that basolateral sorting signals of various basolateral proteins, such as MCT3/MCT4,

operate differently in MDCK and RPE cells.<sup>42,13</sup> In MDCK cells and intestinal cells, CLC-2 displays a basolateral distribution, guided by well-defined basolateral signals that interact with clathrin adaptor AP-1.<sup>27</sup> In this report, we find that HA-tagged CLC-2 localizes to the apical surface of RPE cells in mouse retina. Experiments in human fetal RPE and ARPE-19 cells further confirm the apical polarity of CLC-2 (Caceres et al, in preparation). The reversed polarity of surface proteins in RPE, relative to most other cell types, is a frequent observation not fully explained mechanistically yet. For example,  $Na^+/K^+$ -ATPase and MCT1 are apical in RPE cells, whereas they are targeted to the basolateral membrane in epithelia of the kidney and small intestine.<sup>13,43</sup> In the case of  $Na^+/K^+$ -ATPase, the change in localization appears to depend on the glycosylation of the beta subunit associated with the functional alpha subunit.<sup>44</sup> In the case of MCT1, the change in localization from basolateral in kidney cells to apical in RPE cells depends on the lack of recognition of basolateral signals in basigin, the chaperone protein of MCT transporters.<sup>45</sup> The signals that drive CLC-2 to the apical surface of RPE cells are still

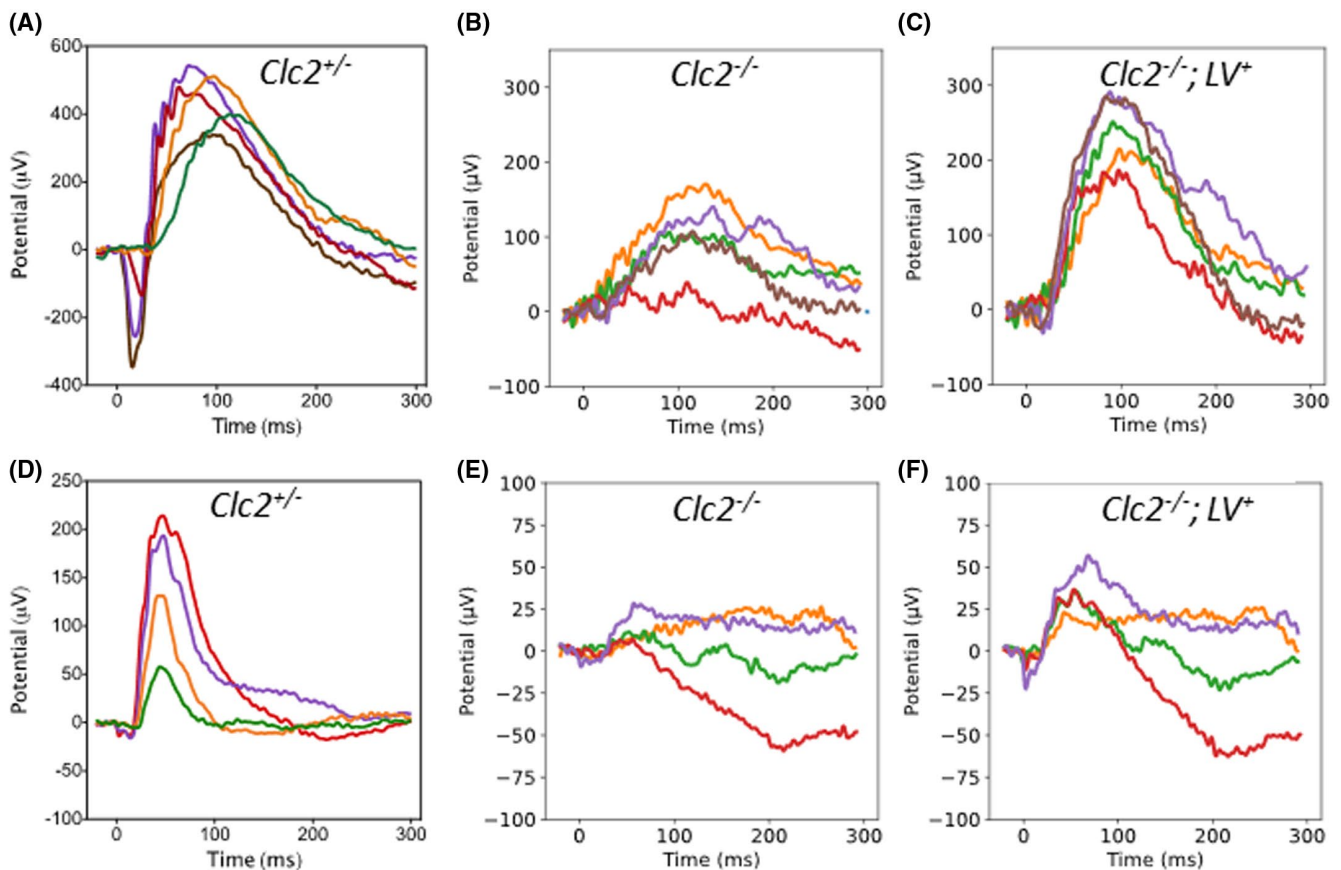


**FIGURE 7** ERG measurements in lentiviral-transduced and untransduced eyes in  $CLC-2^{-/-}$  mice. Scotopic (A-C, n (het) = 6, n (KO) = 8) and photopic ERGs (D-F, n (het) = 6, n (KO) = 7) were measured after lentiviral injection at 6-8 weeks post injection. With light stimuli (see methods for more details), ERG traces, both in the dark and under light, presented a distinctive A-wave and B-wave signature after re-expression of HA-tagged CLC-2 in right eye of homozygous knockouts ( $CLC-2^{-/-}; LV+$ ) (C and E), whereas the untransduced control eye presents only a subtle signal at the brightest light stimulation (B and D). A and D show characteristic scotopic and photopic ERG traces from untransduced heterozygote controls. Dimmest to brightest stimuli coded as: green, orange, red, purple and brown. Red, orange, green, purple, brown

unknown. It is possible, albeit unlikely, that the same signals that drive CLC-2 to the basolateral surface of intestinal and kidney cells, based on dileucine motifs, control its apical localization in RPE cells. It is also unlikely that the characteristic lack of clathrin adaptor AP-1B in RPE cells, which determines the change of basolateral to apical localization of Coxackie Adenovirus Receptor (CAR) in RPE cells, explains the apical localization of CLC-2 as its dileucine-based basolateral signals recognize both AP-1B (lacking in RPE cells) and AP-1A, present in RPE cells. Further investigations are needed to explain the mechanisms involved in apical targeting of CLC-2 in RPE.

Knockout of CLC-2 disrupts the development of the outer retina but affects only slightly the development of the inner retina (Figure 1). CLC-2 is expressed in both photoreceptors and RPE, according to various databases. Hence, lack of CLC-2 might cause photoreceptor degeneration through intrinsic lethal effects of its lack of expression in photoreceptors. This does not seem the case, as RPE-specific transduction of CLC-2 into RPE cells rescues retinal degeneration both structurally (Figure 6) and functionally (Figure 7). Furthermore, RPE-specific knockout of CLC-2 is sufficient to cause retinal degeneration, as recently demonstrated by a recent publication by Jentsch and coworkers that came out while this manuscript was in preparation.<sup>40</sup> Our surprising finding that CLC-2 is expressed apically in RPE cells provides a possible explanation for these findings. The apical localization of CLC-2, in combination with the dramatic retinal degeneration caused by CLC-2 KO in RPE and the rescue of outer retina degeneration by RPE-specific CLC-2 transduction, suggest that apical CLC-2 performs a critical function necessary for the survival of both RPE and photoreceptors. As the composition of the subretinal needs to be kept within limits for the function and survival of photoreceptors, it is logical to postulate that CLC-2 plays a key role in regulation of the normal ionic composition of the subretinal space. Given that CLC-2 is a chloride channel, it may be postulated that its main function is the regulation of the chloride composition of the subretinal space. Our reconstitution experiments show that RPE-specific CLC-2 expression in *CLC-2*<sup>-/-</sup> mouse RPE cells is sufficient to rescue the morphology of both photoreceptors and RPE cells, even when only a fraction of RPE cells are infected and expresses CLC-2-HA. This provides additional support for the idea that apical CLC-2 in RPE cells is in charge of regulating the environment of both RPE and photoreceptors, rather than an intrinsic function of RPE cells where it is necessary for survival of each individual RPE cell.

In this study we show that in absence of CLC-2, the apical localization of MCT1 is drastically perturbed in RPE cells, however the MCT1 localization was restored after lentiviral re-expression of CLC-2 in the RPE monolayer. Studies in mice knocked-out for basigin, a chaperone for lactate transporters, and other proteins, demonstrated that the consequent disruption in the targeting of MCT1 to the apical membrane

compromised the energy level (eg, insufficient lactate transport) in the outer retina, eventually leading to photoreceptor degeneration.<sup>11,46,47</sup> Hence, changes in the apical localization of MCT1 might contribute to the retinal degeneration observed in CLC-2 KO mice. Alternatively, the disrupted MCT1 localization may be a product of a general loss of RPE polarity, which is suggested by the abundant inclusions of ZO-1 at P14. ZO-1 inclusions are a hallmark of the loss of epithelial polarity.<sup>48,49</sup> If the absence of CLC-2 impairs ion and metabolite composition of the subretinal fluid, this harsh microenvironment could trigger a complex reorganization of the RPE where MCT1 is simply one of many bystanders altered in distribution.

As discussed in Introduction, current models for fluid transport in RPE cells postulate a critical role of chloride ions as a main driver of fluid transport. According to these models, chloride intake from the subretinal space is mediated by the cotransporter NKCC1, driven by Na<sup>+</sup> gradients established by the energy dependent Na<sup>+</sup>/K<sup>+</sup>-ATPase.<sup>13,14,19</sup> CLC-2 and/or other Cl<sup>-</sup> channels postulated to be localized to the basolateral membrane (eg, CFTR), are candidates to mediate Cl<sup>-</sup> efflux toward the choroidal circulation.<sup>15-18,20-23,30,50</sup> Our finding that CLC-2 localizes preferentially to the apical membrane suggests that it is not the basolateral channel for efflux of Cl<sup>-</sup> ions. The model for fluid transport needs to be modified to accommodate the expression of a Cl<sup>-</sup> channel at the apical surface.

## ACKNOWLEDGMENTS

We thank Ying Hao of the Duke Eye Center Electron Microscopy Core Facility for her technical assistance, Patrick Zager for his technical assistance in maintaining mouse colony, Paulo S Caceres for his technical assistance of lentivirus preparation, and Diego Gravotta for scientific input. Funding for this study was provided by National Institutes of Health grants EY08538 and GM34107, as well as the NYSTEM contract C32596GG (E.R-B), I.B. was supported by the Comunidad Autónoma de Madrid (grant 2017-T1/BMD-5247); additional grant support from the Research to Prevent Blindness and Dyson Foundation to the Ophthalmology department. Further, the CNIC is supported by the Instituto de Salud Carlos III (ISCIII), the Ministerio de Ciencia e Innovación (MCIN) and the Pro CNIC Foundation. This work was supported by Visual Function Core at Weill Cornell Medicine and the Core grant EY005722 at Duke University.

## CONFLICT OF INTEREST

The authors declare no competing financial interest.

## AUTHOR CONTRIBUTIONS

C. Hanke-Gogokhia, G.L. Lehmann, I. Benedicto, E. de la Fuente-Ortega, R. Schreiner, and E. Rodriguez-Boulan designed the research. C. Hanke-Gogokhia, G.L. Lehmann,

and R. Schreiner performed the research. I. Benedicto and E. de la Fuente-Ortega contributed to new reagents or analytic tools. C. Hanke-Gogokhia and R. Schreiner analyzed the data. C. Hanke-Gogokhia, V.Y. Arshavsky, R. Schreiner, and E. Rodriguez-Boulan wrote the paper.

## ORCID

Ryan Schreiner  <https://orcid.org/0000-0002-7457-6606>  
 Enrique Rodriguez-Boulan  <https://orcid.org/0000-0003-2033-6233>

## REFERENCES

- Singh RK, Nasonkin IO. Limitations and promise of retinal tissue from human pluripotent stem cells for developing therapies of blindness. *Front Cell Neurosci.* 2020;14:179.
- Strauss O. The retinal pigment epithelium in visual function. *Physiol Rev.* 2005;85:845-881.
- Bonilha VL, Finnemann SC, Rodriguez-Boulan E. Ezrin promotes morphogenesis of apical microvilli and basal infoldings in retinal pigment epithelium. *J Cell Biol.* 1999;147:1533-1548.
- Raymond SM, Jackson IJ. The retinal pigmented epithelium is required for development and maintenance of the mouse neural retina. *Curr Biol.* 1995;5:1286-1295.
- German OL, Buzzi E, Rotstein NP, Rodriguez-Boulan E, Politi LE. Retinal pigment epithelial cells promote spatial reorganization and differentiation of retina photoreceptors. *J Neurosci Res.* 2008;86:3503-3514.
- Longbottom R, Fruttiger M, Douglas RH, Martinez-Barbera JP, Greenwood J, Moss SE. Genetic ablation of retinal pigment epithelial cells reveals the adaptive response of the epithelium and impact on photoreceptors. *Proc Natl Acad Sci USA.* 2009;106:18728-18733.
- Nasonkin IO, Merbs SL, Lazo K, et al. Conditional knockdown of DNA methyltransferase 1 reveals a key role of retinal pigment epithelium integrity in photoreceptor outer segment morphogenesis. *Development.* 2013;140:1330-1341.
- Jablonski MM, Tombran-Tink J, Mrazek DA, Iannaccone A. Pigment epithelium-derived factor supports normal development of photoreceptor neurons and opsin expression after retinal pigment epithelium removal. *J Neurosci.* 2000;20:7149-7157.
- Mazzoni F, Safa H, Finnemann SC. Understanding photoreceptor outer segment phagocytosis: use and utility of RPE cells in culture. *Exp Eye Res.* 2014;126:51-60.
- Hamann S. Molecular mechanisms of water transport in the eye. *Int Rev Cytol.* 2002;215:395-431.
- Lakkaraju A, Umopathy A, Tan LX, et al. The cell biology of the retinal pigment epithelium. *Prog Retin Eye Res.* 2020;78:100846.
- Rizzolo LJ. Development and role of tight junctions in the retinal pigment epithelium. *Int Rev Cytol.* 2007;258:195-234.
- Lehmann GL, Benedicto I, Philp NJ, Rodriguez-Boulan E. Plasma membrane protein polarity and trafficking in RPE cells: past, present and future. *Exp Eye Res.* 2014;126:5-15.
- Caceres PS, Rodriguez-Boulan E. Retinal pigment epithelium polarity in health and blinding diseases. *Curr Opin Cell Biol.* 2020;62:37-45.
- Kennedy BG. Na(+)-K(4)-Cl- cotransport in cultured cells derived from human retinal pigment epithelium. *Am J Physiol.* 1990;259:C29-C34.
- Miller SS, Edelman JL. Active ion transport pathways in the bovine retinal pigment epithelium. *J Physiol.* 1990;424:283-300.
- Bialek S, Joseph DP, Miller SS. The delayed basolateral membrane hyperpolarization of the bovine retinal pigment epithelium: mechanism of generation. *J Physiol.* 1995;484(Pt 1):53-67.
- Hu JG, Gallemore RP, Bok D, Frambach DA. Chloride transport in cultured fetal human retinal pigment epithelium. *Exp Eye Res.* 1996;62:443-448.
- Caceres PS, Benedicto I, Lehmann GL, Rodriguez-Boulan EJ. Directional fluid transport across organ-blood barriers: physiology and cell biology. *Cold Spring Harb Perspect Biol.* 2017;9:a027847. <https://doi.org/10.1101/cshperspect.a027847>
- Jentsch TJ. CLC chloride channels and transporters: from genes to protein structure, pathology and physiology. *Crit Rev Biochem Mol Biol.* 2008;43:3-36.
- Thiemann A, Grunder S, Pusch M, Jentsch TJ. A chloride channel widely expressed in epithelial and non-epithelial cells. *Nature.* 1992;356:57-60.
- Grunder S, Thiemann A, Pusch M, Jentsch TJ. Regions involved in the opening of CIC-2 chloride channel by voltage and cell volume. *Nature.* 1992;360:759-762.
- Pena-Munzenmayer G, Catalan M, Cornejo I, et al. Basolateral localization of native CIC-2 chloride channels in absorptive intestinal epithelial cells and basolateral sorting encoded by a CBS-2 domain di-leucine motif. *J Cell Sci.* 2005;118:4243-4252.
- Jentsch TJ. Chloride transport in the kidney: lessons from human disease and knockout mice. *J Am Soc Nephrol.* 2005;16:1549-1561.
- Bosl MR, Stein V, Hubner C, et al. Male germ cells and photoreceptors, both dependent on close cell-cell interactions, degenerate upon CIC-2 Cl(-) channel disruption. *EMBO J.* 2001;20:1289-1299.
- Edwards MM, Marin de Evsikova C, Collin GB, et al. Photoreceptor degeneration, azoospermia, leukoencephalopathy, and abnormal RPE cell function in mice expressing an early stop mutation in CLCN2. *Invest Ophthalmol Vis Sci.* 2010;51:3264-3272.
- de la Fuente-Ortega E, Gravotta D, Perez Bay A, et al. Basolateral sorting of chloride channel 2 is mediated by interactions between a dileucine motif and the clathrin adaptor AP-1. *Mol Biol Cell.* 2015;26:1728-1742.
- Wang H, Xu M, Kong Q, et al. Research and progress on CIC2 (Review). *Mol Med Rep.* 2017;16:11-22.
- Arreola J, Melvin JE. A novel chloride conductance activated by extracellular ATP in mouse parotid acinar cells. *J Physiol.* 2003;547:197-208.
- Nehrke K, Arreola J, Nguyen HV, et al. Loss of hyperpolarization-activated Cl(-) current in salivary acinar cells from Clcn2 knockout mice. *J Biol Chem.* 2002;277:23604-23611.
- Mattapallil MJ, Wawrousek EF, Chan CC, et al. The Rd8 mutation of the Crb1 gene is present in vendor lines of C57BL/6N mice and embryonic stem cells, and confounds ocular induced mutant phenotypes. *Invest Ophthalmol Vis Sci.* 2012;53:2921-2927.
- Qiao X, Pennesi M, Seong E, Gao H, Burmeister M, Wu SM. Photoreceptor degeneration and rd1 mutation in the grizzled/mocha mouse strain. *Vision Res.* 2003;43:859-865.
- Lobanova ES, Herrmann R, Finkelstein S, et al. Mechanistic basis for the failure of cone transducin to translocate: why cones are never blinded by light. *J Neurosci.* 2010;30:6815-6824.
- Spencer WJ, Ding JD, Lewis TR, et al. PRCD is essential for high-fidelity photoreceptor disc formation. *Proc Natl Acad Sci USA.* 2019;116:13087-13096.

35. Ding JD, Salinas RY, Arshavsky VY. Discs of mammalian rod photoreceptors form through the membrane evagination mechanism. *J Cell Biol.* 2015;211:495-502.
36. Lobanova ES, Finkelstein S, Herrmann R, et al. Transducin gamma-subunit sets expression levels of alpha- and beta-subunits and is crucial for rod viability. *J Neurosci.* 2008;28:3510-3520.
37. Zhang K, Liu GH, Yi F, et al. Direct conversion of human fibroblasts into retinal pigment epithelium-like cells by defined factors. *Protein Cell.* 2014;5:48-58.
38. Seandel M, Butler JM, Kobayashi H, et al. Generation of a functional and durable vascular niche by the adenoviral E4ORF1 gene. *Proc Natl Acad Sci USA.* 2008;105:19288-19293.
39. Venkatesh A, Ma S, Langelotto F, Gao G, Punzo C. Retinal gene delivery by rAAV and DNA electroporation. *Curr Protoc Microbiol.* 2013;28. <https://doi.org/10.1002/9780471729259.mc14d04s28>
40. Goppner C, Soria AH, Hoegg-Beiler MB, Jentsch TJ. Cellular basis of CIC-2 Cl(-) channel-related brain and testis pathologies. *J Biol Chem.* 2020;296:100074.
41. Marmorstein AD, Marmorstein LY, Rayborn M, Wang X, Hollyfield JG, Petrukhin K. Bestrophin, the product of the Best vitelliform macular dystrophy gene (VMD2), localizes to the basolateral plasma membrane of the retinal pigment epithelium. *Proc Natl Acad Sci USA.* 2000;97:12758-12763.
42. Castorino JJ, Deborde S, Deora A, et al. Basolateral sorting signals regulating tissue-specific polarity of heteromeric monocarboxylate transporters in epithelia. *Traffic.* 2011;12:483-498.
43. Philp NJ, Wang D, Yoon H, Hjelmeland LM. Polarized expression of monocarboxylate transporters in human retinal pigment epithelium and ARPE-19 cells. *Invest Ophthalmol Vis Sci.* 2003;44:1716-1721.
44. Lobato-Alvarez JA, Roldan ML, Lopez-Murillo TD, Gonzalez-Ramirez R, Bonilla-Delgado J, Shoshani L. The apical localization of Na(+), K(+)-ATPase in cultured human retinal pigment epithelial cells depends on expression of the beta2 subunit. *Front Physiol.* 2016;7:450.
45. Deora AA, Philp N, Hu J, Bok D, Rodriguez-Boulan E. Mechanisms regulating tissue-specific polarity of monocarboxylate transporters and their chaperone CD147 in kidney and retinal epithelia. *Proc Natl Acad Sci USA.* 2005;102:16245-16250.
46. Philp NJ, Ochrietor JD, Rudoy C, Muramatsu T, Linsler PJ. Loss of MCT1, MCT3, and MCT4 expression in the retinal pigment epithelium and neural retina of the 5A11/basigin-null mouse. *Invest Ophthalmol Vis Sci.* 2003;44:1305-1311.
47. Han JYS, Kinoshita J, Bisetto S, et al. Role of monocarboxylate transporters in regulating metabolic homeostasis in the outer retina: Insight gained from cell-specific Bsg deletion. *FASEB J.* 2020;34:5401-5419.
48. Engevik AC, Krystofiak ES, Kaji I, et al. Recruitment of polarity complexes and tight junction proteins to the site of apical bulk endocytosis. *Cell Mol Gastroenterol Hepatol.* 2021;12:59-80. <https://doi.org/10.1016/j.jcmgh.2021.01.022>
49. Hurd TW, Gao L, Roh MH, Macara IG, Margolis B. Direct interaction of two polarity complexes implicated in epithelial tight junction assembly. *Nat Cell Biol.* 2003;5:137-142.
50. Kane Dickson V, Pedi L, Long SB. Structure and insights into the function of a Ca(2+)-activated Cl(-) channel. *Nature.* 2014;516:213-218.

## SUPPORTING INFORMATION

Additional Supporting Information may be found online in the Supporting Information section.

**How to cite this article:** Hanke-Gogokhia C, Lehmann GL, Benedicto I, et al. Apical CLC-2 in retinal pigment epithelium is crucial for survival of the outer retina. *The FASEB Journal.* 2021;35:e21689. <https://doi.org/10.1096/fj.202100349R>